

Hunting for the progenitor of SN 1006: High resolution spectroscopic search with the FLAMES instrument¹

Wolfgang E. Kerzendorf^{1,2}, Brian P. Schmidt¹, John B. Laird³, Philipp Podsiadlowski⁴,
Michael S. Bessell¹

wkerzend@mso.anu.edu.au

ABSTRACT

Type Ia supernovae play a significant role in the evolution of the Universe and have a wide range of applications. It is widely believed that these events are the thermonuclear explosions of carbon-oxygen white dwarfs close to the Chandrasekhar mass ($1.38 M_{\odot}$). However, CO white dwarfs are born with masses much below the Chandrasekhar limit and thus require mass accretion to become Type Ia supernovae. There are two main scenarios for accretion. First, the merger of two white dwarfs and, second, a stable mass accretion from a companion star. According to predictions, this companion star (also referred to as donor star) survives the explosion and thus should be visible in the center of Type Ia remnants. In this paper we scrutinize the central stars (79 in total) of the SN 1006 remnant to search for the surviving donor star as predicted by this scenario. We find no star consistent with the traditional accretion scenario in SN1006.

1. Introduction

Type Ia supernovae (SNe Ia) have applications in a wide range of astronomical fields. Their iconic use as cosmological distance probes which enabled the discovery of the accelerated expansion of the universe is augmented by their role as major drivers of chemical evolution in the universe. They are also physically interesting endpoints of stellar evolution. It is therefore an embarrassment that the progenitors of these explosion are as yet unknown.

The spectra and light curves of SNe Ia suggest that the explosion is powered by burning

of degenerate carbon-rich matter, suggesting carbon/oxygen white dwarfs as progenitors of SN Ia. These objects provide carbon-rich degenerate matter and self ignite as they approach the Chandrasekhar mass threshold ($1.38 M_{\odot}$). Most white dwarfs, however, are born with $0.6 M_{\odot}$, and how they reach the required threshold is as of yet unknown. Two main scenarios have been identified by the community (Iben 1997). The first channel involves the merger of two white dwarfs (double-degenerate scenario) with a total mass above the Chandrasekhar limit and explosive nucleosynthesis of the merger product. In the second channel, mass is accreted from a non-degenerate companion (single-degenerate scenario). Close to the Chandrasekhar limit, explosive carbon burning ensues and the white dwarf undergoes a thermonuclear detonation/deflagration. This scenario offers an important calling card: the survival of the non-degenerate companion (also known as donor star).

Our lack of understanding about the progenitor channel has significant impact on our understanding of the chemical evolution of the Universe. Thus, the community has put considerable effort into uncovering the progenitor scenario (for a review see Kerzendorf et al. 2012, *subm.*). A direct

¹Research School of Astronomy and Astrophysics, Mount Stromlo Observatory, Cotter Road, Weston Creek, ACT 2611, Australia

²Department of Astronomy and Astrophysics, University of Toronto, 50 Saint George Street, Toronto, ON M5S 3H4, Canada

³Department of Physics & Astronomy, Bowling Green State University, Bowling Green, OH 43403, USA

⁴Department of Astrophysics, University of Oxford, Oxford, OX1 3RH, United Kingdom

¹Based on observations collected at the European Organisation for Astronomical Research in the Southern Hemisphere, Chile (ESO 083.D-0805(A))

detection of a surviving donor star in a Galactic Type Ia remnant would substantiate the single degenerate channel for at least one system.

The community has identified several Galactic Type Ia remnants that lend themselves to search for the surviving donor star (RCW86, SN 1006, SN 1572 and SN 1604). In this paper, we have chosen SN 1006 for a spectroscopic search of the inner stars. The lack of a central neutron star, observations of several tenths of a solar mass of iron inside the remnant (Hamilton et al. 1997), the high peak luminosity and basic light curve shape (visible for several years; Goldstein & Peng Yoke 1965) all indicate that SN 1006 was a SN Ia. The remnant has a secure distance, measured by Winkler et al. (2003), who combined the proper motion and the radial velocity of the expanding shell to measure the distance to 2.2 kpc, making SN 1006 the closest of the Galactic SN Ia remnants (consistent with SN 1006 being the brightest). The geometric centre of the remnant is well determined from both X-ray and radio observations (Winkler et al. 2003).

The interior of the remnant has been probed with UV background sources (Winkler et al. 2005), which revealed the aforementioned iron core as well as a silicon-rich shell (adding to the evidence that SN 1006 was a SN Ia event). In addition, the remnant has been searched previously for possible objects associated with the supernova explosion, which revealed an unusual O-star (Schweizer-Middleditch Star (henceforth SM-Star); Schweizer & Middleditch 1980) that was suggested as a possible remnant star to SN 1006. After successful identifications of neutron stars in both the Vela Remnant and the Crab Remnant this was thought to be the third identification of a stellar remnant in a historical supernova. Subsequent UV spectroscopic follow-up of the Schweizer-Middleditch star (SM-Star) by Wu et al. (1983) showed strong Fe II lines with a profile broadened by a few thousand km s^{-1} and symmetrically distributed around the rest-wavelength. In addition, Wu et al. (1983) identified redshifted Si II, Si III and Si IV lines. Their conclusion was that these absorption lines stem from the remnant and place the SM-Star behind the remnant, making it unrelated to SN 1006. The SM-Star remains an ideal object to probe the remnant and measure upper limits for interstellar extinction $E(B-V) = 0.1$ (Wu et al. 1993; Winkler

et al. 2003).

SN 1006 has several properties which make it well suited for a progenitor search. Although the remnant is the oldest among the remnants with a secure Type Ia identity, its age is still young enough that the remnant's centre is well determined, and the motion of any potential donor star is low enough that only a small area needs to be searched. Furthermore, the elapse of 1005 years is a short length of time relative to the timescales of stellar evolution for donor stars (see Marietta et al. 2000) so we still expect a potential donor star to be close to the same state as directly after the supernova explosion. In addition, SN 1006 has a low interstellar extinction, which eases the determination of stellar parameters. Finally, with 2.2 kpc it is the closest of the known SN Ia remnants and thus is suitable for a relatively deep survey. These serendipitous conditions for the SN 1006 remnant led us to launch a photometric and spectroscopic campaign to search for the donor star.

In Section 2 we outline the observations as well as data reduction of the photometric and spectroscopic data. Section 3 is split into three subsections, namely radial velocity, stellar rotation and stellar parameters. We discuss our findings in Section 4 and conclude our work in Section 5.

2. Observations and Data Reduction

2.1. Photometric Observations

CCD images of the central $6'$ of the SN 1006 remnant were obtained using the imaging camera at the Nasmyth-B focus of the ANU 2.3 m Telescope at the Siding Spring Observatory on 11 May 2004. The camera has a $6'$ diameter circular field with a scale of $0.375''/\text{pixel}$. We used the broadband Bessell UBVI filters and exposed for 1860 s in U, 1490 s in B, 788 s in V and 1860 s in I. For calibration purposes we took images of the PG1633 and PG1047 standard star regions (Landolt 1992) in the same filters. The seeing ranged between $1''$ and $2''$, and the conditions were photometric. The data were bias corrected and flatfielded (with skyflats) using PYRAF² and IRAF³.

²PyRAF is a product of the Space Telescope Science Institute, which is operated by AURA for NASA.

³IRAF: the Image Reduction and Analysis Facility is distributed by the National Optical Astronomy Observatory,

For our photometric data reduction we fitted an astrometric solution using the astrometry from the 2MASS point source catalogue (Skrutskie et al. 2006) to our frames. We used SExtractor (Bertin & Arnouts 1996) to measure the magnitudes of the objects in the frames (using a $2''$ aperture), corrected for atmospheric extinction and then we calibrated our photometry to the standard Johnson-Cousins UBV(Ic) system using the Stetson magnitudes⁴ of the stars in the standard fields PG1633+099 and PG1047+003 (Landolt 2009). The measured magnitudes were supplemented with near infrared magnitudes from the 2MASS point source catalogue (see online tables).

We have also computed temperatures from photometric colours by using the polynomials given in Casagrande et al. (2010). In the first instance, we assumed a solar metallicity for all stars, but the choice of metallicity only has a relatively minor influence on the temperature determination, for example, using B-V there is a change of less than 200 K for metallicities between $[\text{Fe}/\text{H}]=0$ and $[\text{Fe}/\text{H}]=-1$, while for V-K and V-I there is virtually no change. All temperatures are provided in online tables.

2.2. Spectroscopic Observations

For the spectroscopy survey we used the Very Large Telescope (VLT) instrument FLAMES, which can provide high-resolution ($R = 25,000$) optical spectra over a $25'$ field of view for up to 130 objects. In this mode, the spectral coverage is limited to 200 \AA . We chose the wavelength region from 5139 \AA to 5356 \AA which contains the gravity sensitive Mg I b triplet as well as many iron lines, to accurately measure metallicity. For the centre of our spectroscopic survey we chose the mean of the X-ray and radio centre ($\alpha = 15^{\text{h}}02^{\text{m}}22^{\text{s}}.1$ $\delta = -42^{\circ}05'49''$; Winkler et al. 2003). We do note that the center choice is one of the most problematic choices in a progenitor search. Particularly, measurements by Winkler et al. (2005) cast doubt on a precise determination of the centre of SN 1006. Their research suggests that the

which is operated by the Association of Universities for Research in Astronomy (AURA) under cooperative agreement with the National Science Foundation (NSF).

⁴This research used the facilities of the Canadian Astronomy Data Centre operated by the National Research Council of Canada with the support of the Canadian Space Agency

centre of the iron core is offset from the geometric centre determined by the shocked interstellar medium (ISM). However, we argue that this does not mean that the centre of mass (where a donor star would reside) is necessarily off centre. In fact, Maeda et al. (2010) suggest that the iron ejecta is offset from the centre of mass, which suggests that the centre of the iron core will be different from the centre of mass. In general, explosion models are consistent with the center of mass being given by the outer shock, not the iron core. In addition, we chose a generous search radius of $120''$, corresponding to the motion of a star travelling 1250 km s^{-1} at 2.2 kpc over 1000 years. This choice, which is more than four times the maximum expected escape velocity of the donor from the system (Han 2008), was made to accommodate any errors in the choice of the centre. Although the models predict the surviving companion to be several hundred L_{\odot} (Marietta et al. 2000), we chose a limiting magnitude of $V = 17.5$ ($0.5 L_{\odot}(V)$ at 2.2 kpc including reddening of $E(B-V)=0.1$; see Equation 1) to accommodate a wide range of potential donor star scenarios.

$$L_{\odot}(V) = 10^{-0.4(V-4.83)+1.24 \cdot E(B-V)} 4.8 \times 10^4 \frac{d}{2.2 \text{ kpc}}^2 \quad (1)$$

An exposure time of 3.8 hours was chosen to obtain spectra with high enough quality to measure rotation and basic stellar parameters (S/N ratio > 20). For completeness and so to not waste fibres we chose additional stars down to a magnitude limit of $V = 19$ only to be used for radial velocity measurements. There are 26 stars with $V < 17.5$ and 53 stars with $17.5 < V < 19$ mag (for a total of 79 stars) for our survey (see Figure 1). With fibre buttons not being able to be placed less than $11''$ apart, we had to split our candidates over three different setups. The first two setups were observed five times for 2775 s each. We deliberately chose bright stars for the last setup so that it only had to be observed three times for 2775 s each. In addition, we placed spare fibres on three bright stars ($R \approx 10$; 2MASS J15032744-4204463, 2MASS J15031746-4204165, 2MASS J15033195-4202356) located close to the edge of the $25'$ field of view for calibration purposes. Additional spare fibres were placed on sky positions, which were chosen to be far from 2MASS sources and manually inspected on DSS images to be in star free

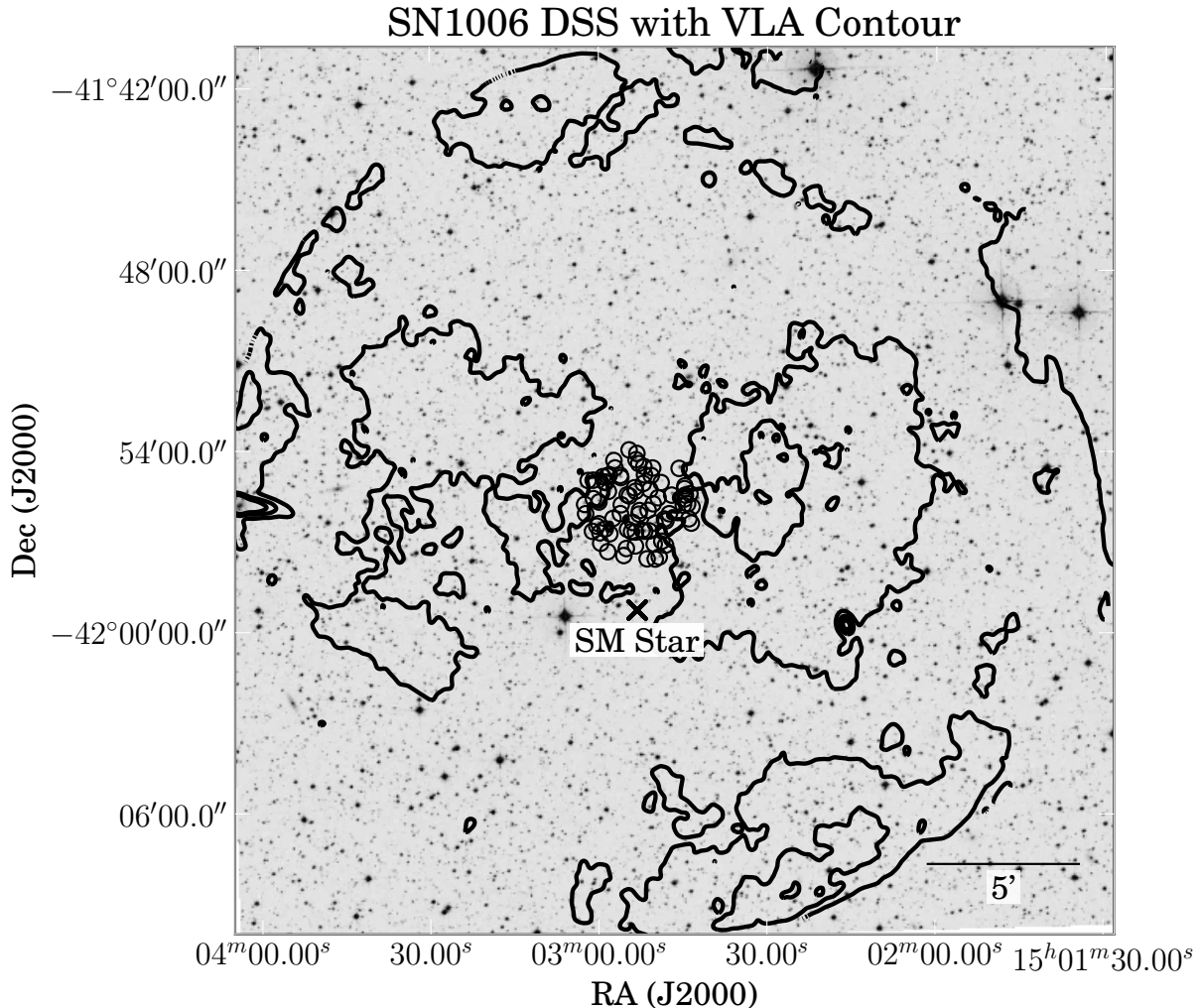


Fig. 1.— Optical DSS image with radio contour overlay (VLA data from Moffett et al. 1993). The black circles in the centre show the 79 program stars. Additionally we have marked the ‘spurious’ donor the Schweizer-Middleditch star.

regions. In addition to our nighttime calibration, which included simultaneous arc exposures with four fibres for each observation block, we received standard daytime calibrations. In total, 13 observation blocks with an exposure time of 2775 s each were obtained. Table 1 provides the Observing ID, modified Julian date, mean seeing, mean airmass, setup name and heliocentric correction for all observations (all data are available under ESO Program ID: 083.D-0805(A)). Due to broken

fibres, not all stars were observed for the expected length of time. Broken fibres caused SN1006-31 not to be observed at all in this project (see Figure 2), although with $V = 17.87$, SN1006-31 is not part of our primary sample and thus not crucial for our search.

We first applied a cosmic ray removal tool on the raw 2D frames (van Dokkum 2001). The data were then reduced with the ESO-CPL pipeline (version 5.2.0), using the GIRAFFE instrument

Table 1: FLAMES Observations of SN1006 program stars

ObsID	MJD	FWHM	Airmass	Setup name	v_{helio} correction
-	d	"	-	-	km s ⁻¹
360737	54965.1	1.2	1.2	SN1006 1	1.5
360739	54965.1	1.2	1.1	SN1006 1	1.5
360740	54965.1	1.0	1.1	SN1006 1	1.4
360741	54985.0	0.7	1.4	SN1006 1	-7.4
360742	54964.2	1.5	1.1	SN1006 1	1.7
360743	54985.0	0.8	1.2	SN1006 2	-7.5
360745	54985.0	0.9	1.1	SN1006 2	-7.6
360746	54985.1	1.0	1.1	SN1006 2	-7.7
360747	54985.1	1.0	1.1	SN1006 2	-7.7
360748	54985.2	0.9	1.1	SN1006 2	-7.8
360749	54963.1	1.2	1.2	SN1006 3	2.4
360751	54963.1	1.1	1.1	SN1006 3	2.3
360752	54963.2	1.1	1.1	SN1006 3	2.3

recipes (version 2.8.9). The only variation that was made to the default parameters was the usage of the Horne extraction algorithm instead of the ‘‘Optimal’’-extraction algorithm. This yielded 366 individual spectra of the candidate stars and an additional 39 calibration star spectra.

3. Analysis

3.1. Radial Velocity

To obtain radial velocities we employ a two-step process. We first cross correlated each spectrum with a solar spectrum from Kurucz et al. (1984) using the standard technique described in Tonry & Davis (1979) and implemented in the PYRAF task FXCOR. The cross-correlation was performed on each individual spectrum. In the second step, heliocentric corrections were applied and then the results were averaged for each star with a sigma clipping algorithm (for candidate stars with $V < 17.5$ see Table 2; the radial velocities of all stars are available online). We note that especially for faint objects we observe a second cross-correlation peak at 0 km s⁻¹ and suspect that this stems from scattered moonlight. We believe that this has a negligible effect on our radial velocity measurement. In Figure 3 we compared our radial velocity measurements with the Besançon kinematic model of the Milky way (Robin et al. 2003). Our selection criteria from the Besançon kinematic model was

all stars within 1 square degree of SN 1006 and a magnitude cut of $10 < V < 17.5$. We compared the resulting 10000 stars to our 78 stars in the sample in Figure 3. All stars are consistent with what is expected from the Besançon model and show no irregularities attributable to donor star candidates.

3.2. Rotational Velocity

Kerzendorf et al. (2009) suggest that a previously unrealized feature of donor stars is high rotation. Contrary to the predicted radial velocity signature which can be submerged in the velocity distribution of the Galaxy, the rotational velocities of stars is normally less than 10 km s⁻¹ for late-type stars and the predicted high rotational velocities of donor stars should be clearly distinguishable. The measured rotational velocity includes a factor of $\sin i$. However, the expected rotational velocities are above $v_{\text{rot}} = 50$ km s⁻¹ and thus we still expect to see modest rotation even with a high inclination angle.

We have measured the rotational velocity of the stars of the $V < 17.5$ candidate stars using a cross-correlation technique (Carney et al. 1987). First, we cross-correlated the stars with a synthetic spectrum matching closest in T_{eff} , $\log g$ and $[\text{Fe}/\text{H}]$ space (and a intrinsic rotational velocity of $v_{\text{rot}} = 2$ km s⁻¹). If the cross-correlation peak was

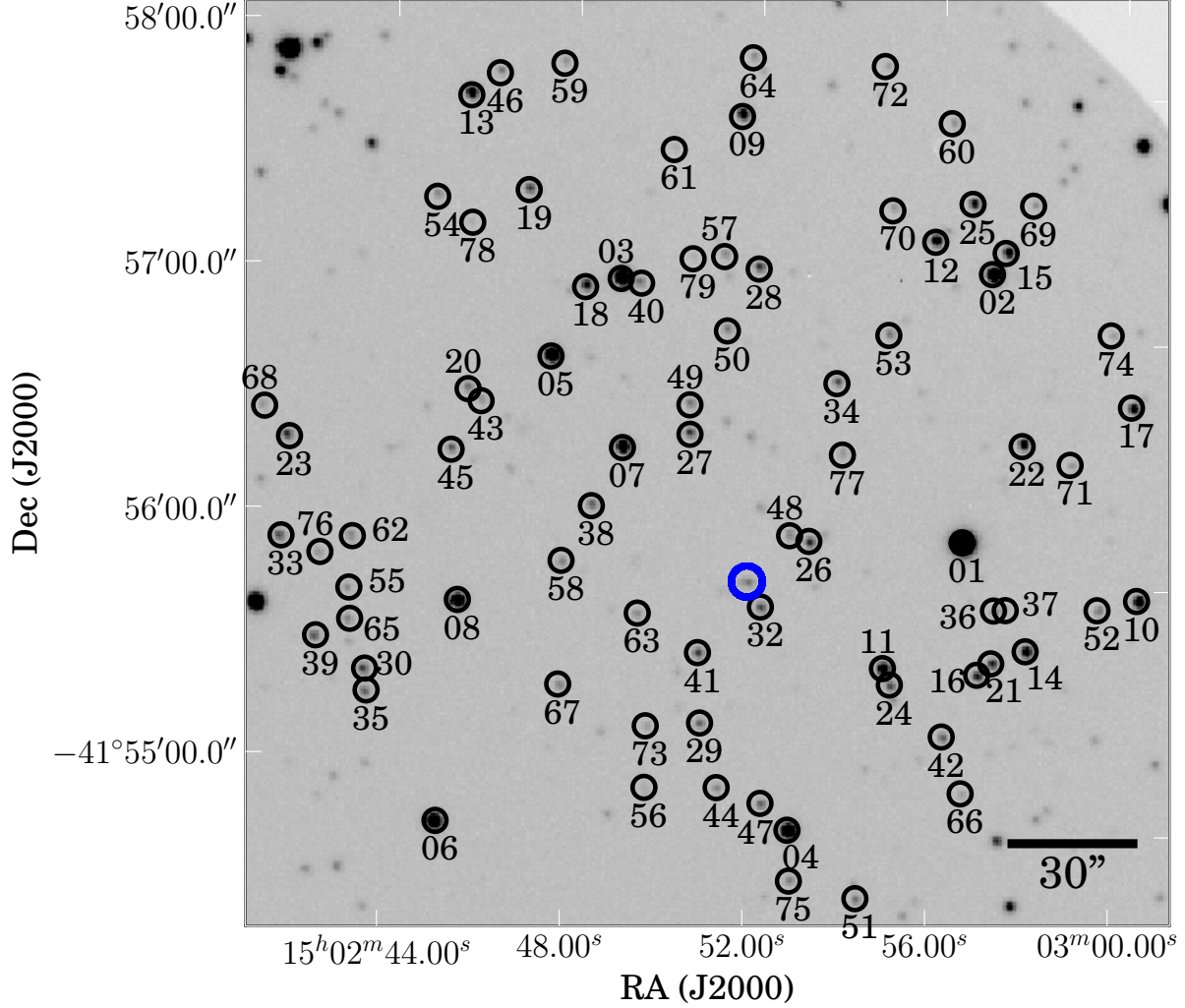


Fig. 2.— V-Band image taken by the 2.3 m Telescope. We have marked SN1006-31, which was not observed due to broken fibres, with a blue circle. With a brightness of $V = 17.87$, SN1006-31 is fainter than our primary catalog ($V < 17.5$ mag), and is the only star which lacks a spectrum to $V = 19$ mag in the remnant’s centre.

broader than expected from instrumental resolution ($\approx 12 \text{ km s}^{-1}$), we attributed the extra broadening to rotation. This should yield the qualitatively correct result, although there may be significant systematic errors (due to other broadening effects, however $< 5 \text{ km s}^{-1}$). However, our main goal is to identify rotators with $v_{\text{rot}} > 30 \text{ km s}^{-1}$,

which this technique does with a high degree of confidence. The resulting estimates of $v_{\text{rot}} \sin i$ are given in Table 2.

3.3. Stellar Parameters

We obtained detailed stellar parameters for the donor candidates with $V < 17.5$ by employing

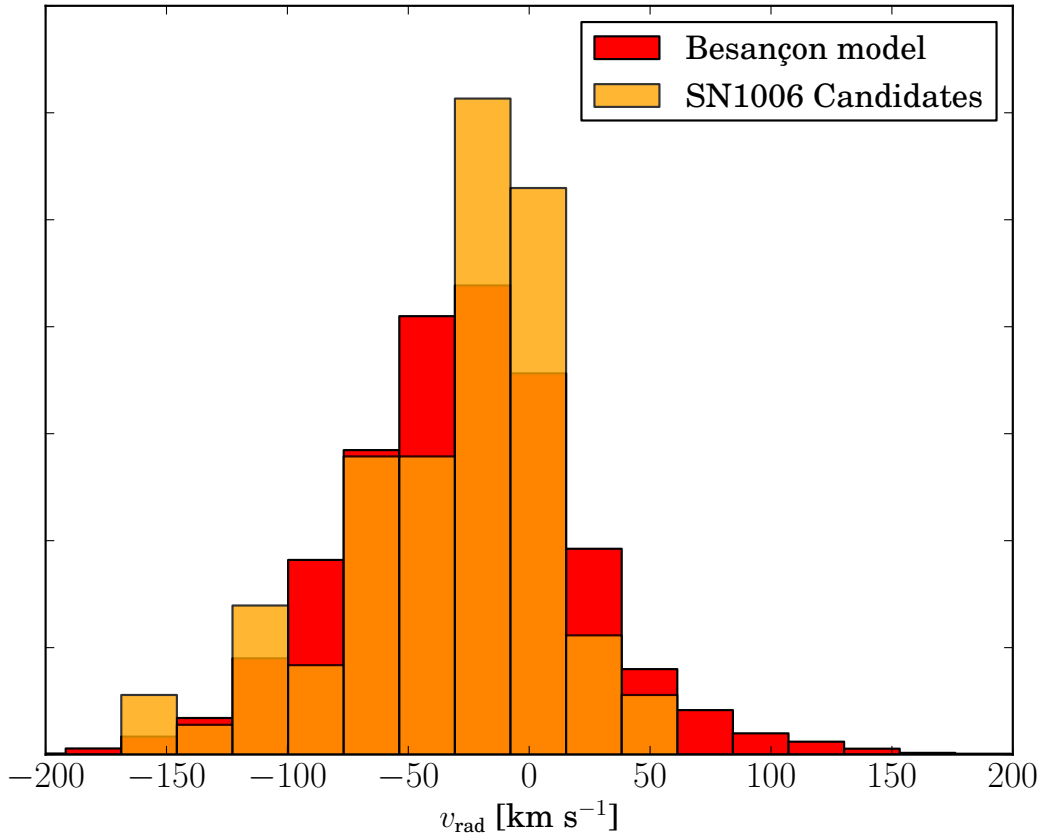


Fig. 3.— Comparison of all candidate stars with the distribution of stars taken from the the Besançon kinematic model. The model input parameters were a search area of 1 square degree around the centre of SN 1006 and a magnitude limit of $10 < V < 17.5$

a grid-based technique with a three-dimensional grid in T_{eff} , $\log g$ and $[\text{Fe}/\text{H}]$. MOOG (Snedden 1973) was used to synthesise the spectral grid using the model stellar atmospheres by Castelli & Kurucz (2003). Line wings were taken into account up to 8 Å away from the line centre, which seemed to be a reasonable compromise between grid creation time and accuracy. For the atomic lines we merged values from the Vienna Atomic Line Database (VALD; Kupka et al. 2000) with adjusted values (to reproduce the Arcturus and the Sun) from Gustafsson et al. (2008). In addition, we used the measured molecular lines described in Kurucz & Bell (1995). The final grid extends from 3500 K to 7500 K in effective temperature with a

step size of 250 K, from 0 to 5 in surface gravity with a stepsize of 0.5, from -2.5 to 0.5 in $[\text{Fe}/\text{H}]$ with a stepsize of 0.5 (with an extra set of points at 0.2).

We used the appropriate sections from the Solar spectrum (Kurucz et al. 1984) and the Arcturus spectrum (Hinkle et al. 2000) to calibrate our spectral grid. We measured stellar parameters by first finding the best fitting grid point and then using the minimizer MINUIT to find a minimum by interpolating between the gridpoints (Barber et al. 1996). For the Sun we obtain stellar parameters of $T_{\text{eff}}=5825$ K, $\log g=4.4$ and $[\text{Fe}/\text{H}]=-0.12$ and for Arcturus we obtain stellar parameters of $T_{\text{eff}}=4336$ K, $\log g=1.9$, $[\text{Fe}/\text{H}]=-$

0.67 (cf. $T_{\text{eff}}=4436$ K, $\log g=1.84$, $[\text{Fe}/\text{H}]=-0.54$; Luck & Heiter 2007). We acknowledge the error in measurement, but believe our spectral grid to be accurate enough for distinguishing a potential donor candidate against an unrelated star (our requirement is to determine $\log g$ to 1 dex and T_{eff} to 1000 K accuracy).

To fit our observed spectra, we first fitted the continuum with Legendre polynomials with a maximum order of 3 and a sigma clipping algorithm to discard the lines. The order that gave the lowest RMS of the fit was adopted. We then combined the spectra using the previously measured radial velocity and the computed heliocentric correction. In addition, we broadened the synthetic spectral grid with a rotational kernel for each star where applicable. These spectra were then fitted using the previously described algorithm, except that we added the $B - V$ photometric temperature as a prior. As the photometric temperature uses the metallicity as an input parameter we recalculated the photometric temperature prior to using the metallicity determined by the fit. This procedure was repeated until the gravity estimate converged to less than 0.1 dex. We believe our temperatures to be good to a few hundred K, and our surface gravities and metallicities have a systematic uncertainty of roughly 0.5 dex (much smaller than our required precision).

The stellar parameters are given in Table 2. The final set of stellar parameters shows a typical distribution of many dwarfs and a few giants. None of the stars seem to be unusual in any way.

4. Discussion

In this work we have scrutinised all stars to a limit of $0.5 L_{\odot}(V)$ at the distance of the SN 1006 remnant. In addition, we have performed radial velocity measurements of stars down to a limit of $\approx 0.1 L_{\odot}(V)$ at the distance of SN 1006. Although theoretical models predicted bright donor stars, we have searched down to relatively faint limits. As these predictions were only theoretical in their nature, it was important further features that could hint at a donor star (namely rotation, radial velocity, and unusual stellar parameters). We used population synthesis models from Han (2008) to judge our rotation measurement with the

the rotation of donor stars post-explosion (see Figure 4). None of the stars scrutinised in our sample show features consistent with those expected in any current donor star models or are significantly unusual.

Giant donor stars are easily ruled out because there is no star bright enough to be at the distance of the remnant. Marietta et al. (2000) suggest that giant donors have a luminosity of $\approx 1000 L_{\odot}$ ($V \approx 9$ at the distance of the remnant) for at least 100,000 years. Furthermore, these models suggest that the giant donor is likely to have a high temperature of more than 10^4 K. In addition, the star should have rotation in excess of what has been measured for any of the stars in this sample. In summary, there is no viable giant star donor star among the stars located in SN 1006.

Subgiant donors should also be very luminous post explosion (Marietta et al. 2000) with a minimum expected luminosity of $L \approx 500 L_{\odot}$ ($V \approx 9.7$ at the distance of the remnant) lasting for 1400 – 11,000 years, although theoretical models allow a much larger variation of this class of stars (Podsiadlowski 2003). While they might have a radial velocity which could be masked by the large expected dispersion in the direction of SN 1006, the expected $v_{\text{rot}} \approx 80 \text{ km s}^{-1}$ (see Figure 4) far exceeds any star in our sample. Therefore, we believe we can confidently rule out sub-giant donor stars in this case as well. In summary our research shows a consistent result to SN 1572 - no identifiable donor star for SN 1006.

Finally, main sequence stars, according to Marietta et al. (2000) are expected to have a similar brightness to subgiant stars, although this enhanced luminosity depends on the details of how energy is deposited from the explosion (see Podsiadlowski 2003). However, main sequence donors should have both substantial spatial motion and a very high rotation. No star, in our sample, shows any of these features and our sample's depth should cover all conceivable post-evolutionary scenarios, even for a main sequence donor star.

One caveat is that rotation can decrease due to expansion (Kerzendorf et al. 2009). However, this should result in a star with a low gravity. No such star is present in SNR 1006.

Table 2: SN 1006 candidates ($V < 17.5$) stellar parameters

Name	T_{eff} K	$\log g$ dex	[Fe/H] dex	V mag	v_{rad} km s $^{-1}$	v_{rot} km s $^{-1}$
01	4285	2.0	-1.0	13.50	-109.1	< 10
02	4001	0.8	-1.4	15.37	56.2	< 10
03	5446	4.0	-0.6	15.04	5.9	< 10
04	5347	4.0	-0.6	15.47	-14.3	< 10
05	5191	3.7	-0.6	15.50	-1.1	< 10
06	5874	4.5	-0.7	15.50	-103.9	< 10
07	4884	4.2	-0.8	15.90	-76.3	< 10
08	5954	4.2	-0.5	15.86	-0.6	< 10
09	4217	3.9	-2.5	16.58	-47.0	< 10
10	5662	4.3	-0.8	16.30	-20.2	10
11	5489	4.1	-0.8	16.33	-5.9	< 10
12	5313	4.4	-0.9	16.39	-59.8	16
13	5114	4.0	-0.7	16.49	12.3	< 10
14	5245	4.3	-0.7	16.56	-17.0	< 10
15	5503	4.2	-0.7	16.63	-72.0	< 10
16	4448	4.0	-1.8	17.26	9.4	14
17	5515	4.4	-1.2	16.66	-102.1	< 10
18	5341	4.1	-0.9	16.77	11.6	12
19	3846	4.1	-2.4	17.39	47.8	17
21	4510	3.1	-1.3	17.36	-18.5	13
22	6448	4.2	-0.4	16.71	-22.9	13
23	4429	4.0	-1.8	17.39	63.3	14
25	6119	4.9	-0.7	17.03	40.7	< 10
26	5619	4.0	-1.1	17.23	-7.0	< 10
27	5336	4.0	-1.3	17.47	-52.0	< 10
28	5379	4.3	-1.1	17.43	-43.5	< 10

5. Conclusions

The observations presented here for SN 1006 are in conflict with the standard SN Ia donor star scenarios, which include accretion onto a white dwarf from a main sequence, subgiant, or giant companion. A few non-standard scenarios survive our observational tests. These include a helium white dwarf as a donor star, which would not be detectable with our observations, although it is not entirely clear that a helium white dwarf would survive the explosion (priv. comm. Rüdiger Pakmor). In addition, Justham (2011) & Di Stefano et al. (2011) suggest that the donor star might evolve and become a white dwarf before the supernova explosion. The delay in explosion is explained by the need to spin-down to reach criti-

cal density in the core of the white dwarf. This would again result in a companion, which is not detectable by our methods. Finally, another possibility is that SNe Ia (or at least SN 1006) do not have donor stars, consistent with a double degenerate scenario (DD-scenario).

6. Acknowledgements

B. P. Schmidt and W. E. Kerzendorf were supported by Schmidt’s ARC Laureate Fellowship (FL0992131).

We would like to thank Zhanwen Han for providing population synthesis data. We would like to thank the anonymous referee for insightful and useful comments.

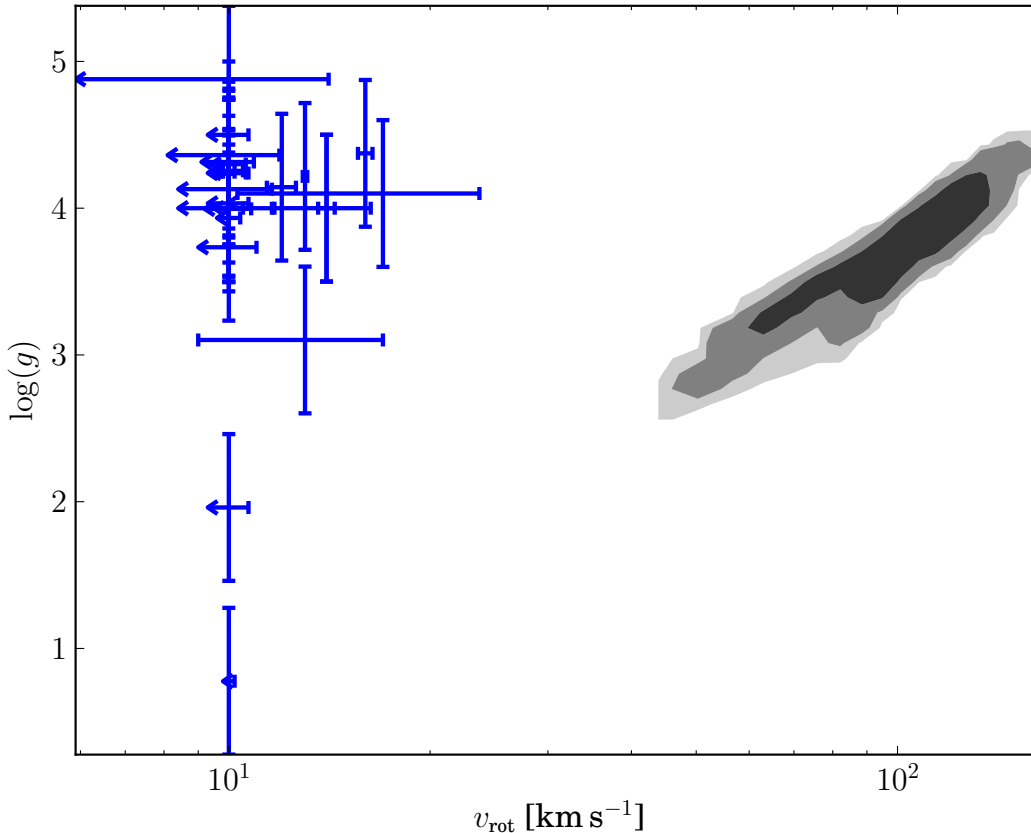


Fig. 4.— Comparison of the evolutionary state and rotational velocity of 55000 binary synthesis SD-Scenario progenitors (gray shades; data from Han 2008) with the measured rotation from this work. Due to the resolution of the spectrograph most of these stars only have an upper limit of the rotation speed of $v_{\text{rot}} = 10 \text{ km s}^{-1}$. In addition, the measurement's are diminished by a factor $\sin i$ which we believe to not change the final result (expected rotation and measured rotation differ by more than a factor of 5).

REFERENCES

- Barber, C. B., Dobkin, D. P., & Huhdanpaa, H. 1996, ACM TRANSACTIONS ON MATHEMATICAL SOFTWARE, 22, 469
- Bertin, E., & Arnouts, S. 1996, A&AS, 117, 393
- Carney, B. W., Laird, J. B., Latham, D. W., & Kurucz, R. L. 1987, AJ, 94, 1066
- Casagrande, L., Ramírez, I., Meléndez, J., Bessell, M., & Asplund, M. 2010, A&A, 512, A54+, 1001.3142
- Castelli, F., & Kurucz, R. L. 2003, in IAU Symposium, Vol. 210, Modelling of Stellar Atmospheres, ed. N. Piskunov, W. W. Weiss, & D. F. Gray, 20P–+
- Di Stefano, R., Voss, R., & Claeys, J. S. W. 2011, ApJ, 738, L1, 1102.4342
- Goldstein, B. R., & Peng Yoke, H. 1965, AJ, 70, 748
- Gustafsson, B., Edvardsson, B., Eriksson, K., Jørgensen, U. G., Nordlund, Å., & Plez, B. 2008, A&A, 486, 951, 0805.0554

- Hamilton, A. J. S., Fesen, R. A., Wu, C.-C., Crenshaw, D. M., & Sarazin, C. L. 1997, *ApJ*, 481, 838, arXiv:astro-ph/9609096
- Han, Z. 2008, *ApJ*, 677, L109, 0803.1986
- Hinkle, K., Wallace, L., Valenti, J., & Harmer, D. 2000, *Visible and Near Infrared Atlas of the Arcturus Spectrum 3727-9300 A*, ed. Hinkle, K., Wallace, L., Valenti, J., & Harmer, D.
- Iben, I. J. 1997, in *NATO ASIC Proc. 486: Thermonuclear Supernovae*, ed. P. Ruiz-Lapuente, R. Canal, & J. Isern (Dordrecht: Kluwer), 111
- Justham, S. 2011, *ApJ*, 730, L34+, 1102.4913
- Kerzendorf, W. E., Schmidt, B. P., Asplund, M., Nomoto, K., Podsiadlowski, P., Frebel, A., Fesen, R. A., & Yong, D. 2009, *ApJ*, 701, 1665, 0906.0982
- Kupka, F. G., Ryabchikova, T. A., Piskunov, N. E., Stempels, H. C., & Weiss, W. W. 2000, *Baltic Astronomy*, 9, 590
- Kurucz, R., & Bell, B. 1995, *Atomic Line Data (R.L. Kurucz and B. Bell) Kurucz CD-ROM No. 23*. Cambridge, Mass.: Smithsonian Astrophysical Observatory, 1995., 23
- Kurucz, R. L., Furenlid, I., Brault, J., & Testerman, L. 1984, *Solar flux atlas from 296 to 1300 nm*, ed. Kurucz, R. L., Furenlid, I., Brault, J., & Testerman, L.
- Landolt, A. U. 1992, *AJ*, 104, 372
- . 2009, *AJ*, 137, 4186, 0904.0638
- Luck, R. E., & Heiter, U. 2007, *AJ*, 133, 2464
- Maeda, K., Taubenberger, S., Sollerman, J., Mazzali, P. A., Leloudas, G., Nomoto, K., & Motohara, K. 2010, *ApJ*, 708, 1703, 0911.5484
- Marietta, E., Burrows, A., & Fryxell, B. 2000, *ApJS*, 128, 615
- Moffett, D. A., Goss, W. M., & Reynolds, S. P. 1993, *AJ*, 106, 1566
- Podsiadlowski, P. 2003, astro-ph/0303660
- Robin, A. C., Reyl e, C., Derri ere, S., & Picaud, S. 2003, *A&A*, 409, 523
- Schweizer, F., & Middleditch, J. 1980, *ApJ*, 241, 1039
- Skrutskie, M. F. et al. 2006, *ApJ*, 131, 1163
- Snedden, C. 1973, *ApJ*, 184, 839
- Tonry, J., & Davis, M. 1979, *AJ*, 84, 1511
- van Dokkum, P. G. 2001, *PASP*, 113, 1420, arXiv:astro-ph/0108003
- Winkler, P. F., Gupta, G., & Long, K. S. 2003, *ApJ*, 585, 324
- Winkler, P. F., Long, K. S., Hamilton, A. J. S., & Fesen, R. A. 2005, *ApJ*, 624, 189, arXiv:astro-ph/0602555
- Wu, C.-C., Crenshaw, D. M., Fesen, R. A., Hamilton, A. J. S., & Sarazin, C. L. 1993, *ApJ*, 416, 247
- Wu, C.-C., Leventhal, M., Sarazin, C. L., & Gull, T. R. 1983, *ApJ*, 269, L5